http://dx.doi.org/10.1016/j.jmatprotec.2018.06.002
This is the Pre-Published Version.

Microstructure evolution of Ti-6Al-2Zr-1Mo-1V alloy and its mechanism in multi-pass flow forming

X.X. Wang [a], M. Zhan [a, *], M.W. Fu [b], P.F. Gao [a], J. Guo [a]

[a] State Key Laboratory of Solidification Processing, School of Materials Science and Engineering, Northwestern Polytechnical University, P.O. Box 542, Xi'an 710072, PR China

[b] Department of Mechanical Engineering, The Hong Kong Polytechnic University, Hung Hom, Kowloon, Hong Kong

[*] Corresponding Author. Tel.: +86-029-88460212-801; Fax: +86-029-88495632; Email: zhanmei@nwpu.edu.cn (M. Zhan)

Abstract

Multi-pass flow forming process is one of the major approaches to producing titanium tubes with thin-walled cross-section in which characteristics of microstructure have a significant effect on accurate geometry and shape forming and desirable properties tailoring. In this study, the microstructure evolution of Ti-6Al-2Zr-1Mo-1V alloy in multi-pass flow forming process is thus systematically studied and the mechanical properties of the spun tube are investigated. The results show that the kinked grains are occurred in the second and third passes then gradually disappeared after the fourth pass. With the compression and shear deformation induced in multi-pass flow forming, non-standard {0002} basal plane texture is formed, which {0002} plane are titled from normal direction (ND) to circumferential direction (CD) and RD with angles of 20° and 30°, respectively. The characteristics of microstructure indicate that α grains are refined by two mechanisms, viz., continuous dynamic recrystallization (CDRX) and deformation-induced intense and localized shearing (DILS). Meanwhile, the grains refined by DILS facilitate further deformation. For primary α grains, grain subdivisions are mainly achieved by DILS under larger shear deformation, while

© 2018 This manuscript version is made available under the CC-BY-NC-ND 4.0 license http://creativecommons.org/licenses/by-nc-nd/4.0/

both CDRX and DILS have a significant effect on secondary α grain refinement during the whole process. Due to the effect of grain refinement, the yield strength of the spun tube in RD and CD is improved by 20.41% and 12.58%, respectively, compared with the initial one. The research thus advances the knowledge about the microstructure evolution mechanisms of Ti-6Al-2Zr-1Mo-1V alloy in flow forming and provides a basis for the microstructure control the properties tailoring of spun tube further.

Keywords: Multi-pass flow forming; Ti-6Al-2Zr-1Mo-1V alloy; Microstructure evolution; Grain orientation; Deformation-induced intense and localized shearing

1. Introduction

Ti-6Al-2Zr-1Mo-1V alloy is as a classical near α titanium alloy (Ti-alloy) [1]. Since it combines the excellent creep behavior of α Ti-alloys with the high strength of α+β Ti-alloys, Ti-6Al-2Zr-1Mo-1V tubes with thin-walled cross-section have been increasingly utilized in various industries, such as aviation, aerospace and military industries [2, 3].

Generally, Ti-alloy tubes with thin-walled cross-section are produced by multi-pass flow forming (or tube spinning) due to the advantages of low forming force, simple tooling and high material utilization. In flow forming process, the blank is displaced axially along a mandrel, while a continuous and localized plastic deformation is applied by the feeding movement of one or more rollers and rotational motion of the mandrel to reduce the thickness of components [4-6]. Based on the directions of material flow and roller traversing, flow forming process can be classified as the forward and backward ones [4]. For the flow forming of Ti-alloy, the forming operations are usually conducted at α+β range. Therefore, the flow forming process of Ti-alloy is one of most applicable thermomechanical processing (TMP) methods to tailor the microstructure while shaping the Ti-alloy components [7-9].

For the Ti-alloys components in TMP, the final properties are mainly dependent on the deformation behavior and microstructure control, which is not only involved the process of dynamic recovery, dynamic recrystallization, globularization and crystallographic texture but also sensitive to the initial microstructure, deformation condition. Weiss et al. [7, 8] and Semiatin et al. [9] reviewed the microstructure evolution and crystallographic texture of the α and α + β Ti-alloys during the TMP, such as rolling and forging, with different forming conditions in detail. Microstructure control and uniformity of deformation can be achieved

with the aid of processing maps and controlling initial microstructure. Gao et al. [10] studied the nonuniform microstructure in the isothermal local loading forming of Ti-6Al-2Zr-1Mo-1V alloy. Then the tri-modal microstructure with well mechanical properties was obtained by the proposed processing scheme of near-β forging followed with conventional forging. Seshacharyulu et al. [11-13] obtained temperature-strain rate window for the Ti-6Al-4V alloy during hot working with higher tensile strength and without microstructural defects based on series researches on the deformation behavior and microstructure mechanism of the Ti-6Al-4V alloy in hot working. Therefore, for the flow forming process, the understanding microstructure evolution is the fundamental and importance to reveal the deformation mechanisms in depth and control the microstructure and further tailor the properties of spun tube.

Recently, investigations on microstructure evolution of Ti-6Al-2Zr-1Mo-1V alloy in spinning process have been reported. Zhan et al. [14] investigated the microstructure homogeneity in shear spinning under different forming conditions. The results showed a final thickness near the value determined by the Sine law and a temperature with in the desired range were the beneficial conditions for obtaining the spun parts with uniform microstructure. In flow forming process, Shan et al. [15] studied the correlation of microstructure inhomogeneity and texture evolution with deformation history in multi-pass flow forming. Their results indicated that kinked and distorted morphology of α grains was generated under the action of compression in the tangent plane of tube. Crystal c axis of α grains of Ti-6Al-2Zr-1Mo-1V alloy was preferred to align with surface normal due to predominant compression in thickness. Chen et al. [16] found that slip deformation was the main

deformation mechanism together with twinning to coordinate the deformation and the recrystallization of primary α phase was the major softening mechanism. Xu et al. [17] focused on the effect of the deformation on microstructure and mechanical properties of spun tube. The tensile strength was increased due to grain refinement and elongation was decreased not only in axial direction but also in circumferential direction. In addition, variations of grain morphology and grain refinement were mentioned in the all previous researches. Therefore, it is concluded that the change of grain morphology, grain orientation and grain refinement are the predominate phenomena for microstructure evolution in the flow forming process of Ti-6Al-2Zr-1Mo-1V alloy, which have significant effect on the final mechanical properties of spun tube. However, quantitative analysis of the grain morphology and grain size, the kernel of grain orientation variation, mechanism of grain refinement and the correlation of these phenomena in flow forming process are not revealed in the previous researches. In other words, there is lack of a systematic and in-depth study on microstructure evolution of near α Ti-alloys in hot flow forming, which would provide a technical guidance for microstructure control and further the quality and properties tailoring of Ti-alloys deformed components.

This study aims at the investigation of the microstructure evolution of Ti-6Al-2Zr-1Mo-1V alloy in multi-pass flow forming process systematically. In tandem with this, the characteristics of grain morphology in each forming pass are investigated first. Then the variation and the kernel of grain orientation, the grain refinement and its mechanism are further revealed and the effect of microstructure evolution on the mechanical properties of the spun tube is also studied.

2. Experiments

2.1 Experimental sample

The blank used in this research is the ring sample of Ti-6Al-2Zr-1Mo-1V and the dimensions are shown in Fig. 1. The chemical composition of the alloy is given in Table 1. The transformation temperature of α/β phase is 998℃. The as-received Ti-alloy ring was rolled at 950℃ and then followed by the annealing at 750℃×2h. To provide a stable contact condition between the rollers and blank at the initial flow forming stage, the blanks are chamfered by 22.5° in accordance with the attacking angle of the rollers. The initial microstructure of blank is shown in Fig. 2, in which the equiaxed primary α phase within the transformed β is observed. The average grain size of the primary α grain is 15.6μm.

Table 1 Chemical composition of Ti-6Al-2Zr-1Mo-1V alloy (mass fraction, %).

Ti	Al	Mo	V	Zr	Si	Fe	C	N	O	H
Bal.	6.62	1.72	2.23	2.26	<0.04	0.03	0.006	0.002	0.11	0.001

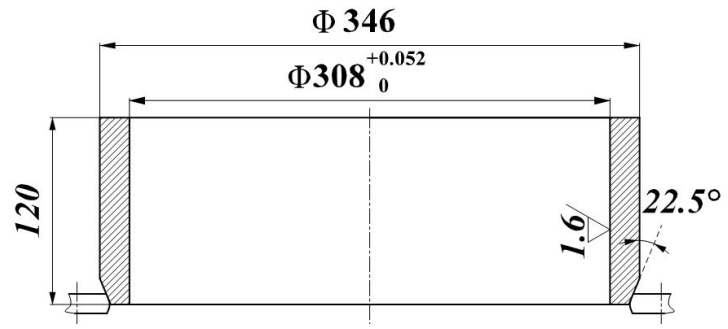

Fig. 1 Dimensons of the flow forming blank.

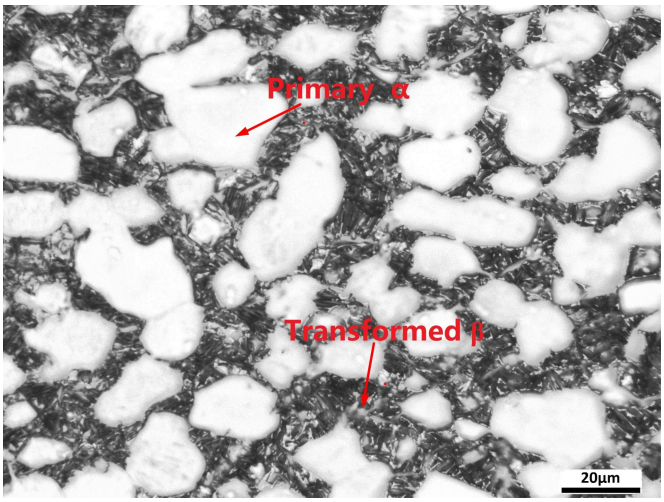

Fig. 2 Initial microstructure of the blank.

2.2 Experimental procedure

The flow forming experiment was carried out on a HO-018 CNC spinning machine with three rollers. The illustration of multi-pass flow forming is shown in Fig. 3. The main forming parameters of the machine are listed in Table 2. Considering the geometry of the billet and the sensitivity of Ti-alloy to crack, backward flow forming technique was adopted in the experiment. Before spinning, the mandrel and billet were preheated to 400 and 800℃, respectively. During the spinning, the billet was heated by two hand-held oxyacetylene flames to maintain the forming temperature within the range of 800-850 ℃. The billet underwent 5 passes and the thickness reduction of each pass is 3mm. Therefore, the thickness reduction ratios after each pass are 15.79, 31.58, 47.37, 63.16, 78.95%, respectively. For the convenience of observing the microstructure in each pass, a stroke of each pass was decreased, as shown in Fig. 3. Upon the spinning, the component was annealed at 750℃ for 2 hours, followed by air cooling to room temperature.

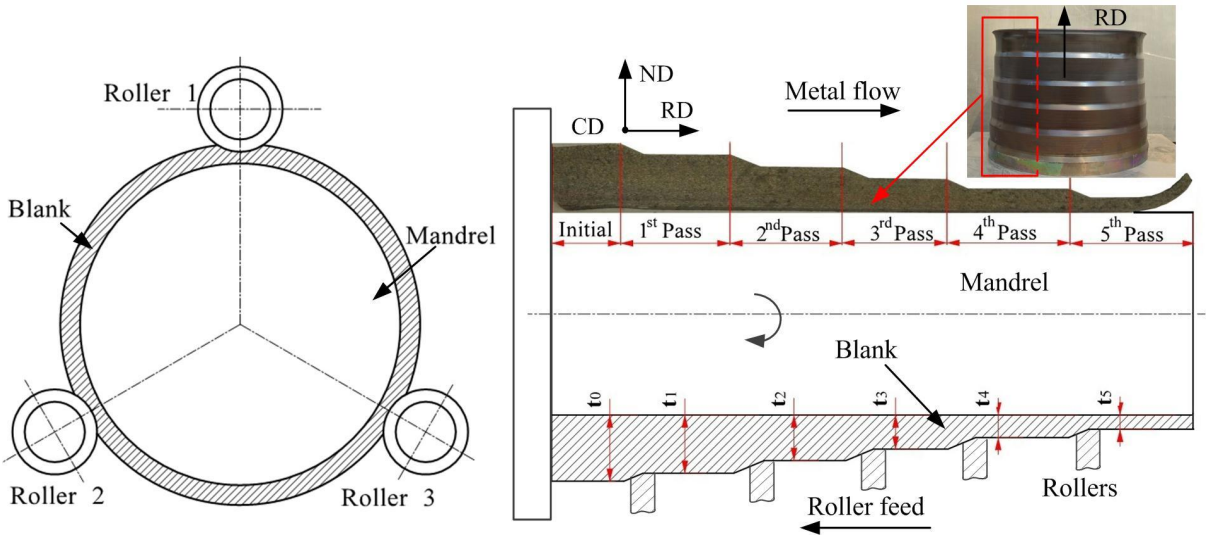

Fig. 3 Illustration of multi-pass flow forming.

Table 2 Main forming parameters in multi-pass flow forming in this study.

Forming parameters	Values
Roller feed rate (mm/r)	1
Mandrel rotation speed (r/min)	89
Forming passes	5
Attacking angle of the roller (°)	22.5
Nose radius of the roller (mm)	8

2.3 Microstructure analysis and mechanical property test

Considering that the main deformation occurs in Rolling-Normal (R-N) plane, as shown in Fig. 3, the microstructure in this plane was observed by optical microscope (OM), electron back-Scattered diffraction (EBSD) and transmission electron microscope (TEM). The procedures for sample preparation and the experimental equipment are shown in Table 3. In EBSD experiments, the images were characterized with the step size of 0.4μm. The grain morphology, grain boundary and crystal orientation were quantified by using the Channel-5

software. To evaluate the mechanical property of spun tube, compression test in rolling direction (RD) and circumferential direction (CD, similar to the transverse direction (TD) in rolling process) was conducted with the sample size of $\varphi 4 \times 6$mm on a ISTRON 3382 mechanical machine.

Table 3 Procedures and equipment for microstructure observation.

Experiment items	Procedures	Equipment
OM	Mechanical grinding + Polishing+ Chemical etching ($80\%H_2O+15\%HNO_3+5\%HF$, 10S)	LEICA DMI3000
EBSD	Mechanical grinding + Electro-polishing ($5\%HClO_4+30\%CH_3OH+65\%C_4H_{10}O$, 28℃, 22V, 40S)	TESCAN
TEM	Mechanical polishing + Double jet polishing ($6\%HClO_4+34\%CH_3OH+60\%C_4H_{10}O$, -20℃, 20V)	H-800

3. Results and discussion

Due to the near α Ti-alloy used in this study and the deformation temperature in the range of 800-850℃, the fraction of α phase was measured to be 83-90% in the microstructure during the flow forming process. Despite of the fact that slip is easy to happen in body-centered cubic (bcc) β phase than hexagonal close-packed (hcp) α phase, the large plastic deformation is insufficiently coordinated by the little β phase and it is mainly coordinated by α phase. These imply α phase has a predominant effect on deformation behavior of Ti-6Al-2Zr-1Mo-1V alloy. The microstructure evolution of α phase is thus the focus for analysis.

3.1 Grain morphology

The microstructure of the spun tube in each pass observed by OM is shown in Fig. 4. It is found that the variation of primary α grains morphology in these images can be characterized well. Upon the first pass spinning, a portion of primary α grains gradually deflects to RD. After the second and third passes, the primary α grains are gradually elongated in the RD and compressed in the normal direction (ND). On the other hand, plenty of elongated α grains are kinked. Such microstructures are also found in compression deformation of Ti-alloy [18]. The complex morphology of primary α grains in flow forming process is caused by the instability of elongated α grains. Since the stability of compression for the elongated α grains is less than that of the equiaxed α grains and deformation area undergoes triaxial compressive stress in flow forming, the increase of compressive stress in RD leads to the generation of kinking of the elongated α grains. When the thickness reduction exceeds 63.16%, most of primary α grains are further compressed and elongated. The stability of compression for α grains is close to each other, which results in the decrease of kinked grains. The axial ratios of primary α grains of the initial billet and the sample after each pass are measured as 2.62, 4.83, 7.84, 9.56, 11.02 and 12.01, respectively. Therefore, the difference values of axial ratio between the neighboring pass are 2.21, 3.01, 2.32, 1.46 and 0.99, respectively. The decrease of the difference value under a larger deformation is resulted from the grain refinement in this case.

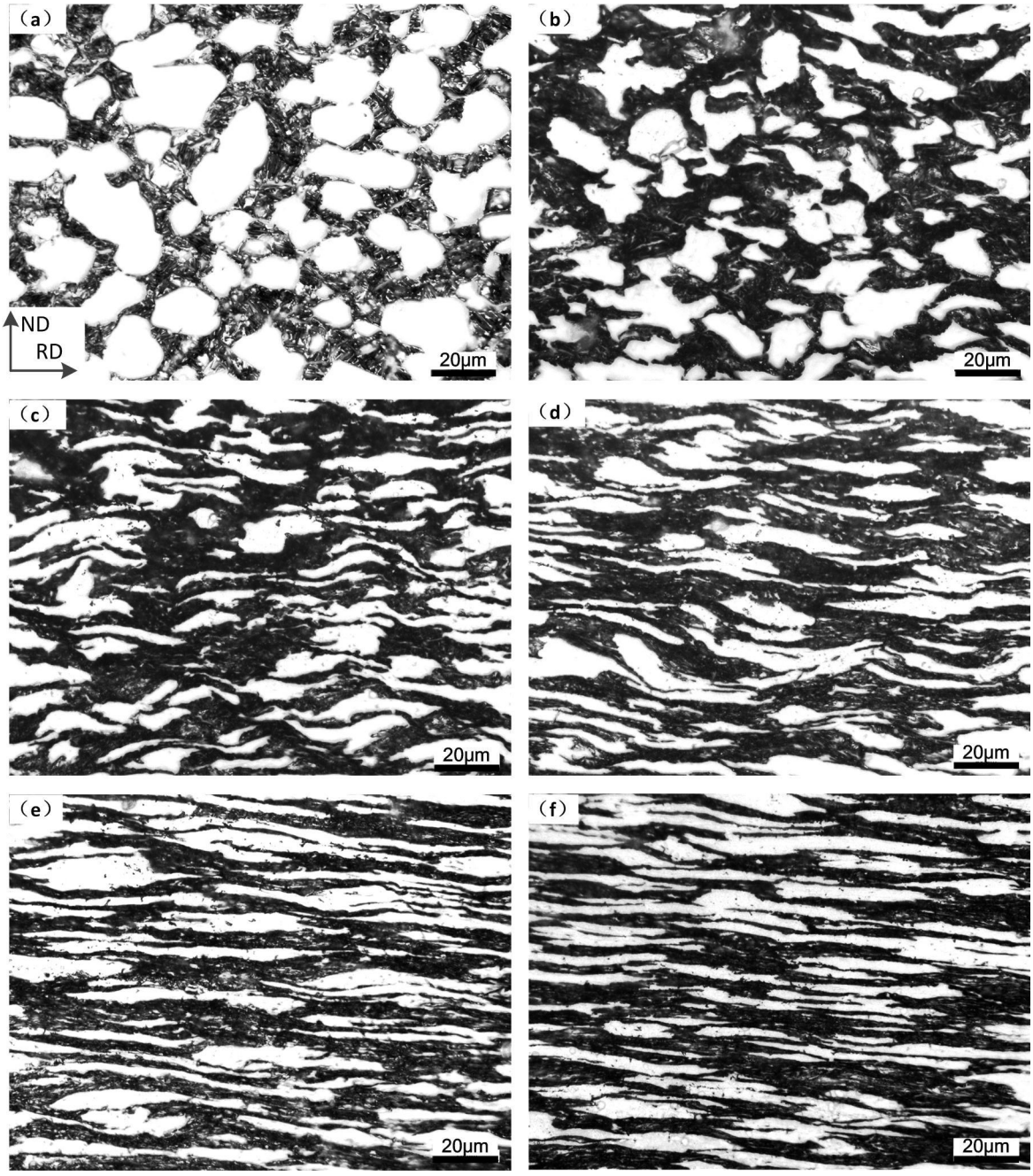

Fig. 4 Grain morphology of the initial billet (a) and the tube spun with the thickness reduction ratio of 15.79% (b), 31.58% (c), 47.37% (d), 63.16% (e) and 78.95% (f).

3.2 Grain orientation

The deflecting of grain morphology to RD in flow forming process will inevitably lead to the change of crystal orientation. Fig. 5 shows the characteristics of grain orientation and crystal rotation with the thickness reduction ratio. In the figure, the ND in the sample

coordinate system is projected to the crystal coordinate system. It is found that in the initial billet, there are different orientations of α grains and the misorientation angle in the interior of α grains is small. Meanwhile, $\{10\bar{1}2\}$ twins are observed, which is resulted from the rolling stage and subsequent annealing heat treatment. Upon the first and second spinning, some secondary α grains are refined with different orientations, as shown in Fig. 5(b)-(c). For the primary α grains, the misorientation in the interior is increased. In addition, many α grains with red color are generated and c axes of these grains are titled towards to ND according to the crystal rotation displayed of grain Ⅰ shown in Fig. 5(c). When the thickness reduction ratio is 47.37 and 63.16%, the c axes of the some refined α grains are also parallel to ND. In some deformed primary α grains highlighted with green and yellow colors, as shown in Fig. 5(e), the misorientaion exists along the straight lines in the interior of the grains. When the thickness reduction ratio is increased to 78.95%, it is noted that the subdivided primary α grains in this case have various colors in addition to the red one, as shown in the white circle of Fig. 5(f). However, most α grains have the same orientation, which reveals the deformation texture is gradually formed with the increase of spinning pass.

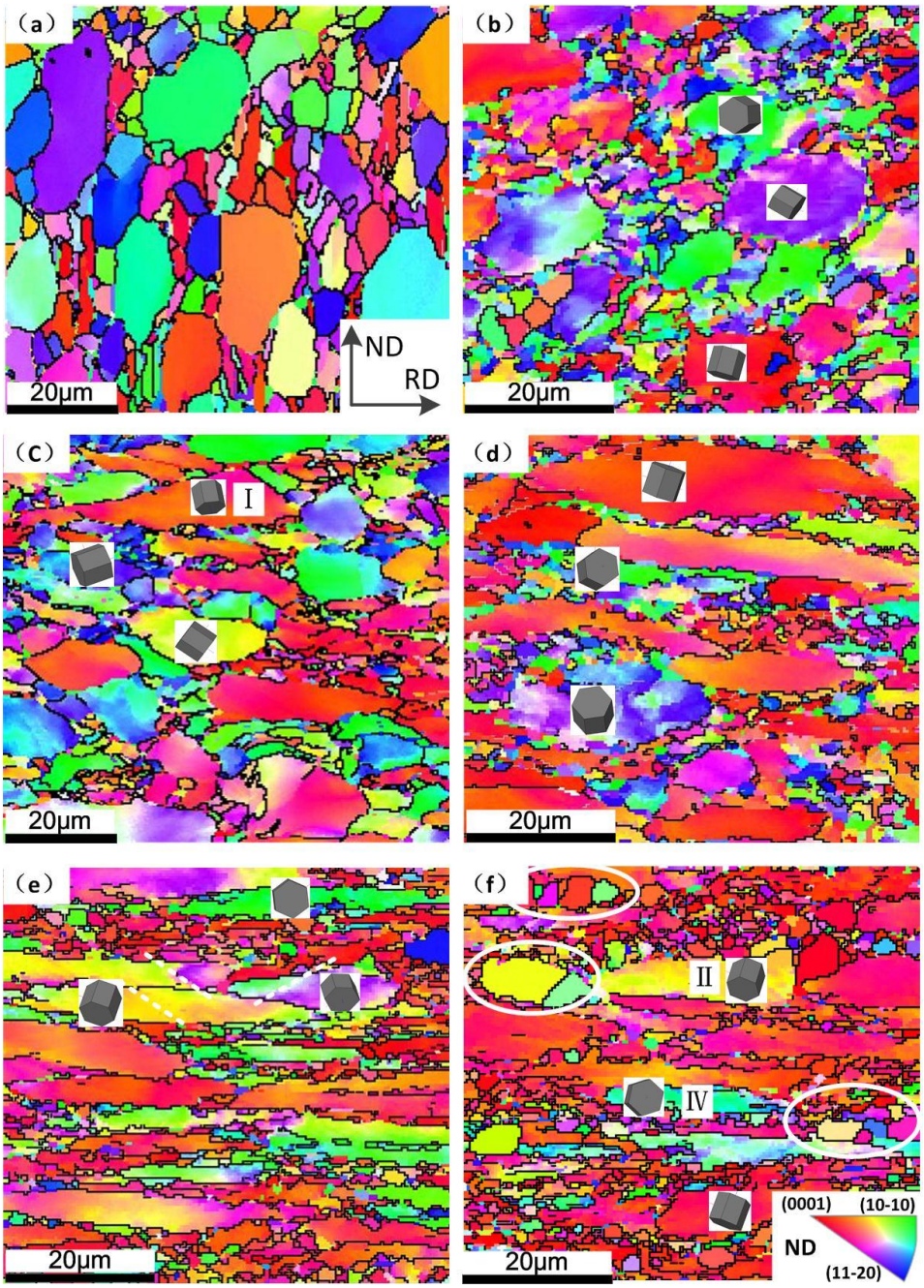

Fig. 5 Grain orientation images of (a) initial billet and the tube spun with the thickness reduction ratio of 15.79% (b), 31.58% (c), 47.37% (d), 63.16% (e), and 78.95% (f).

To reveal the texture evolution in flow forming process, the pole figure is obtained with the thickness reduction, as shown in Fig. 6. It can be seen that, in the initial billet, the $\{0002\}$-poles of α grains are converged on the four points while $\{10\bar{1}0\}$-poles are distributed dispersedly. These indicate that there is recrystallization texture after the previous rolling

process followed with annealing. Upon the first pass spinning, the distribution of {0002}-poles around the circumference indicates that the {0002} planes of α grains are titled to the R-N plane. While the distribution of $\{10\bar{1}0\}$-poles are still dispersive. The intensity of texture is decreased after the first pass since the rotation of substructure induced in flow forming disturbs the preferred orientation of the initial microstructure. With the deformation increasing, the texture corresponding to the grains with red color shown in Fig. 5 is gradually formed and the intensity of texture is increased. In {0002} pole figures, the angle of {0002}-poles with the ND, namely δ, is decreased from 30° to 20° and the angle of {0002}-poles with the CD, namely θ, is always approximately 60°. Meanwhile, the distribution of $\{10\bar{1}0\}$-poles is close to rolling-circumference (R-C) plane. Higher counter lines at point A and B indicate the δ and θ in $\{10\bar{1}0\}$ pole figures are approximately 70° and 60°, respectively. These means that texture generated in flow forming process is not the standard {0002} basal plane texture, or called as c-type texture, which {0002}-poles are parallel to ND [19, 20]. Meanwhile, the deflection angles of {0002}-poles from ND to RD and CD are larger than those of r-type texture which {0002}-poles are tilted some 10° from ND into RD and the $\{10\bar{1}0\}$-poles are parallel to TD and t-type texture {0002}-poles are tilted towards TD and the $\{10\bar{1}0\}$-poles are parallel to RD [20].

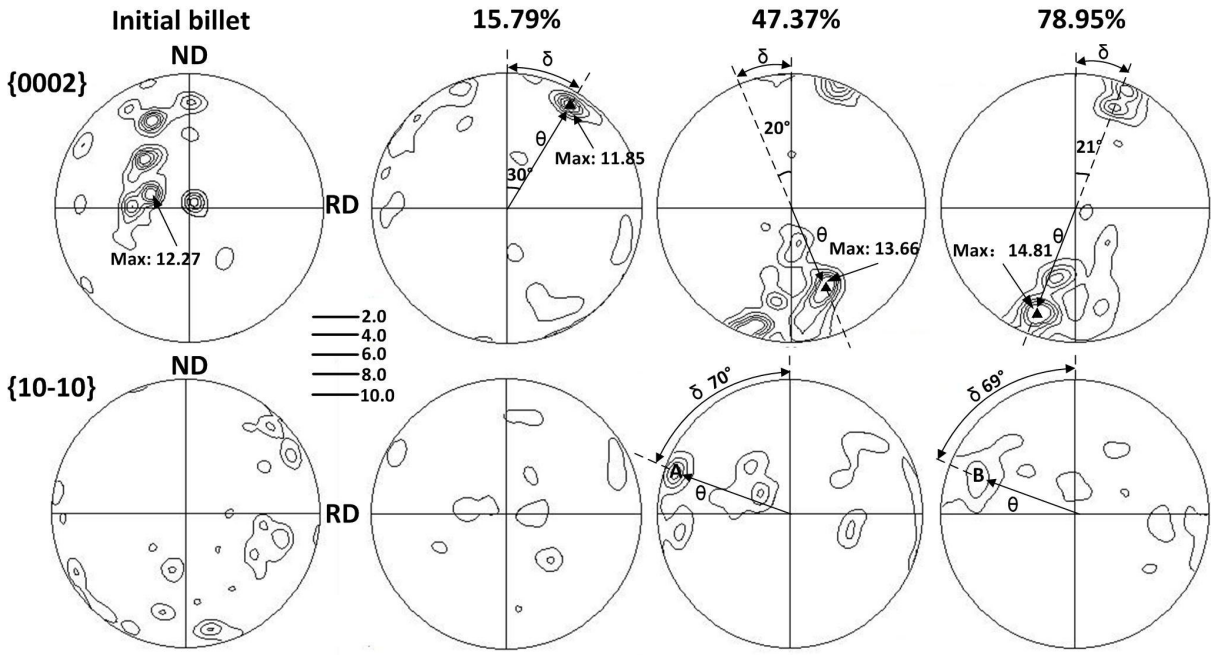

Fig. 6 {0002} and {10$\bar{1}$0} pole figures with the thickness reduction ratio

Crystallographic rotation and texture evolution is associated with the slip and twin systems activated in deformation [19]. The twins only observed in the initial billet indicate that the slip is the main deformation mode in flow forming process of Ti-6Al-2Zr-1Mo-1V titanium alloy. For the α phase, the basal, prismatic and first order pyramidal <a> slip systems, as well as the first and second order pyramidal <a+c> slip systems [21] are shown in Fig. 9(a). The possibility of slip occurring is principally determined by the critical resolved shear stress, τ_c, and Schmid's factors of the slip systems. The τ_c of the <a+c> slip systems is higher than that of the pure <a> deformation systems [19]. The Schmid's factors of the grains corresponding to non-standard {0002} texture, as shown grain Ⅰ in Fig. 5(c), for basal, prismatic and first order pyramidal <a> slip systems are 0.14, 0.011 and 0.099, respectively. These indicate deformation is gradually difficult with the development of the texture due to the low Schmid's factor of <a> slip systems and the higher τ_c for <a+c> slip systems. While the Schmid's factors of the subdivided grains Ⅱ and Ⅳ for basal, prismatic and first order

pyramidal <a> slip systems are 0.5, 0,23, 0.35 and 0.31, 0.44, 0.47, respectively. This means the subdivided grains could be beneficial to the activation of <a> slip systems. Williams et al. [22] have indicated that the prismatic slip provides a lattice rotation about the <0002> direction. Thus, the formation of the non-standard {0002} texture indirectly suggests the preferential activation of prismatic slip in flow forming process. In backward flow forming, the deformation area undergoes the triaxial compressive stress and the stress in ND is the maximum component. Assuming that the prismatic <a> slip system of grain A is activated, for the polycrystalline, the resolved shear stress of <a> slip system projected by compressive stress in ND will generated a moment, which lead to the {0002} basal plane gradually rotated to ND and finally develop the {0002} texture, as shown in Fig. 7(b). The deviation of texture from ND to RD and CD is resulted from significant shear deformation in RD and CD during flow forming process [23].

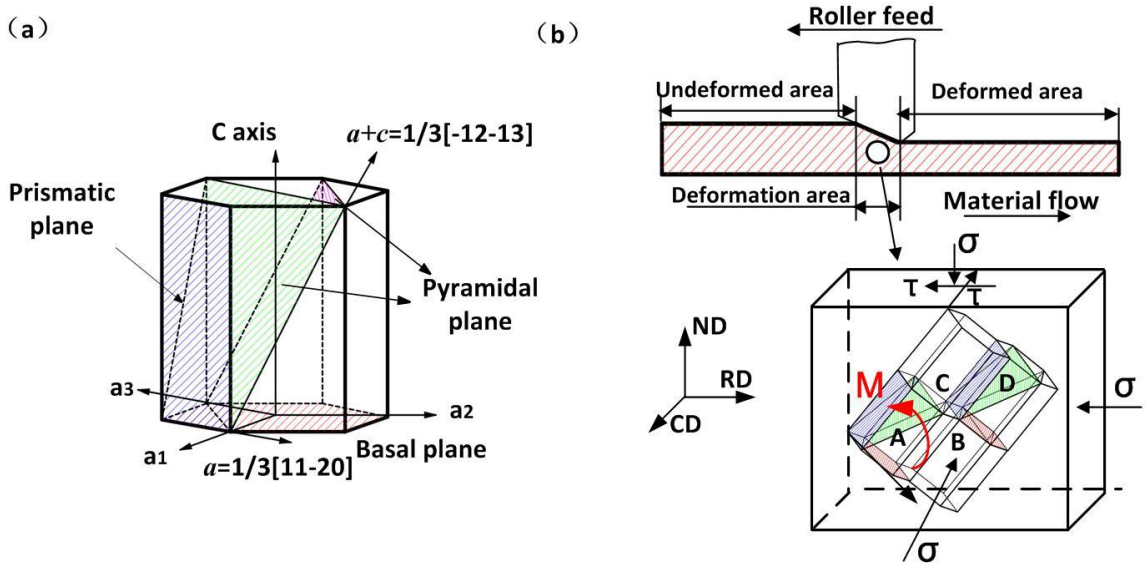

Fig. 7 The slip systems in hcp metals (a), the schematic of crystal rotation in flow forming process

3.3 Grain refinement

Based on the observation of morphology and orientation of α grains articulated above, one prominent phenomenon of microstructure evolution in multi-pass flow forming is the grain refinement, which has also been reported in other spinning process [24, 25]. Therefore, the grain refinement characteristics and its mechanism need to be explored for better microstructure control and property tailoring.

Fig. 8 shows the average value and the standard deviation of grain size with the thickness reduction ratio obtained by EBSD images. It is found that with the increase of deformation, the average grain size and the standard deviation of α grains are decreased linearly. After the fifth pass spinning, the average grain size is approximately 2μm from the original grain size with 3.75μm, which means more refined grains are obtained with the increase of flow forming pass. The larger standard deviation appears due to the big difference in grain size between the coarse primary α grains and the refined secondary α grains.

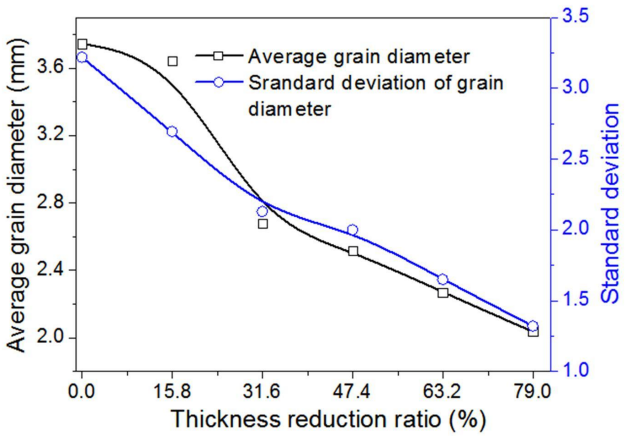

Fig. 8 Percentage of different grain boundaries and average grain size with different thickness reduction ratios

To observe the characteristics of grain refinement after flow forming, grain-subgrain boundary (GSB) images are characterized, as shown in Fig. 9. In the figure, the β phase is

represented by red color, while the α phase is designated by white color. Meanwhile, the green lines represent the low angel boundaries (LABs) (<5°), the red lines refer to the grain boundaries in the range from 5 to 15°. The blue lines designate the high angel boundaries (HABs) (>15°).

In Fig. 9(a), it is found that in the initial annealing ring, a few LABs and grain boundaries in the range from 5 to 15° are mainly distributed in initial coarse grains to form a straight line crossing grains. When the billet is spun after the first pass spinning, as shown in Fig. 9(b), there are some refined grains around the initial coarse grains. It is obviously observed that the proportions of LABs and grain boundaries in the range from 5 to 15° in the α grains are dramatically increased, which are distributed both in primary and secondary α grains. The density of LABs in the interior of grains is smaller than that near the grain boundaries.. Compared with the first pass spinning, the proportion of LABs after the second pass spinning is increased in the primary coarse α grains, as shown in Fig. 9(c). In some primary α grains, as shown in grains Ⅲ and Ⅳ, the LABs cross grains along a straight line. Meanwhile, LABs and HABs are generated and not completely merged or annihilated, as presented in grain Ⅴ in Fig. 9(c). This indicates that continuous dynamic recrystallization (CDRX) is expected to be activated in the primary α grains with the deformation increasing [26, 27]. Combining the grain orientation and GSB images, the grain refinement by CDRX in the flow forming can be explained. First, the misorientation between subgrains is accommodated by high levels of dislocations close to the boundary and then HABs are gradually evolved from the LABs with the increasing of deformation, finally led to their transformation into usual grain boundaries. When the thickness reduction ratio exceeds 47.37%, as shown in Fig.

9(d)-(f), the number of the refined grains is increased with the reduction ratio. The distributions of LABs are mainly concentrated in the un-subdivided primary α grains. In some refined grains, there are LABs and grain boundaries in the range from 5 to 15°, which indicate that these grains are refined by CDRX [28]. However, LABs are not found in other refined grains, which is same as the fragmented primary α grains circled in Fig. 9(f). These mean that there is another mechanism for grain refinement in flow forming process besides CDRX.

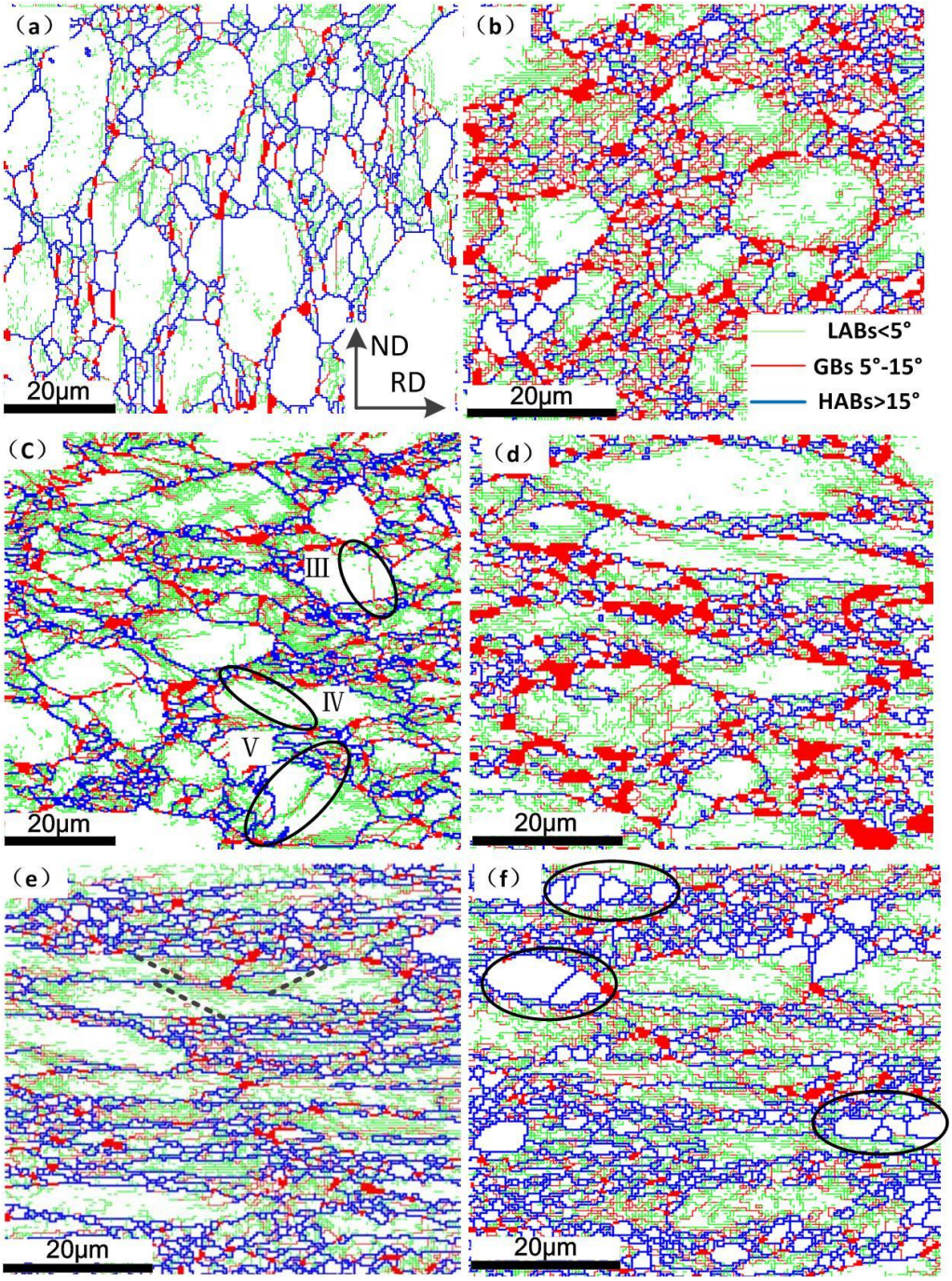

Fig.9 GSB images of the initial billet (a) and tube spun with the thickness reduction ratio of 15.79% (b), 31.58% (c), 47.37% (d), 63.16% (e) and 78.95% (f).

To investigate the other mechanism of grain refinement, substructure images characterized by TEM technique are shown in Fig. 10. In the initial billet, the dislocation density in α phase is relativity low. After the first pass spinning, the dislocation movement induced by deformation results in the formation of dislocation tangle zones (DTZs),

dislocation cells (DCs) and subgrains, as shown in Fig. 10(b). In addition, the DTZs are formed near the grain boundaries and the density of dislocation in the grain boundaries is higher than that in the interior of α grains, which are consistent with the results of EBSD images. Meanwhile, in Fig. 10(b), it shows that some straight lines cross the α lamellae and subdivide the grains, designated by the white circle in the figure. The enlarged image indicates that α lamellae are partially separated along the straight lines. The similar lines are also found in forging of Ti-6Al-4V alloy and termed as the localized shear bands by Weiss et al [8]. And a complete separation of α grains under larger deformation would result in the grain refinement. The process of refinement is also known as globularization. The previous work has identified two ways for globularization during hot deformation [8, 13, 28-30], viz., formation of α/α grain boundaries and penetration of β phase to complete the separation. In one case, the α/α grain boundaries are originated from recrystallization process. The other explanation proposed by Weiss et al. [8] and developed by Seshacharyulu and Zherebtsov et al. [28-30] articulates that α/α grain boundaries are formed by deformation-induced intense and localized shearing (DILS) crossing the α grains. In flow forming process, the significant shear deformation [23] can promote the formation of DILS crossing the α grains. Therefore, the increased deformation contributes to the greater degree of grain refinement by DILS and even formation of the localized ultra-fine grains (UFGs), as shown in Fig. 10(c). When the thickness reduction ratio is increased to 78.95%, most of the deformed α grains are distributed parallel in the β matrix, as shown in 10(d). In the enlarged images, β phase penetrates into α grains along the shear interfaces.

Although the DILS have been observed in α lamellae, the process for the formation of

DILS in α lamellae is difficult to characterize because the separation of α lamellae will be easier even under small deformation [8]. While the process and the characteristics of the refined grains can be characterized well in the primary α grains by combining the EBSD images with TEM images with the deformation increasing.

When the thickness reduction ratio exceeds 31.58%, LABs are formed along the straight lines and the different orientation exists along the lines especially in the elongated α grains with yellow and green colors, as shown in Fig. 10(c)-(d). It reveals that these α grains are rotated to the favorable orientation and the shearing of laths is formed by the intense shear deformation imposed by the rotation of blank and the feed of rollers. Due to the higher Schmid's factors for basal, prismatic and first order pyramidal <a> slip systems for the grains with green and yellow colors, simultaneous recovery by cross-slip is easy to occur, which lead to the annihilation of opposite sign dislocations and leaving groups of dislocations with the same sign to nucleate an interface along the line of shear [13, 28]. Then the rotation of subgrains in the elongated α grains relieves the stress concentration or coordinates the deformation, which promotes the formation of HABs along the shear plane and finally subdivides the grains. Therefore, the subdivided grains have different orientations and without LABs in the interior, as shown in Fig. 5(f). In addition, the orientation of the refined grains formed by DILS is different from most α grains whose basal planes are almost perpendicular to ND. This means grain refinement by DILS can promote the further deformation due to the possibility of slip occurring. The subdivided primary α grains under the larger deformation also indicate that the variation of morphology of primary α grains from equiaxed shape to thicker plate is an important reason for the formation of DILS.

Therefore, grain refinement in flow forming process of Ti-6Al-2Zr-1Mo-1V alloy is achieved by two mechanisms, viz., CDRX and DILS. In the primary α grains, grain subdivision is achieved by CDRX with a small deformation and by DILS with a larger deformation. While for the secondary α lamellae, both mechanisms are important for grain refinement in the whole process.

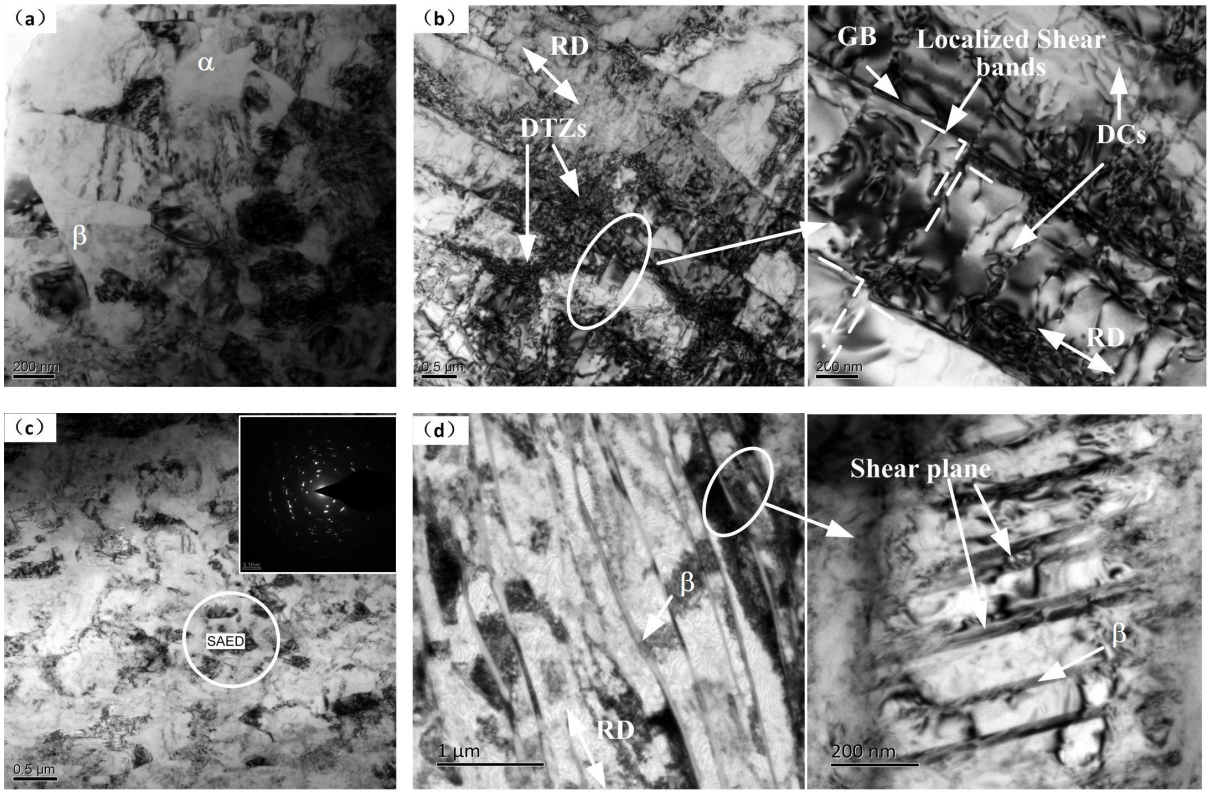

Fig. 8 Grain substructure of the initial billet (a) and the tube spun with the thickness reduction ratio of 15.79% (b), 47.37% (c) and 78.95% (d).

3.4 Mechanical properties of spun tube

Fig. 11 shows the variation of the mechanical property of the spun tube in RD and CD obtained by compression test. The detailed values of yield strength (σ_s) and peak strength are shown in table 4. It is found that both σ_s and peak strength in the two directions are increased with the thickness reduction. Compared with the σ_s of initial billet, the average values of σ_s in RD and CD after five-pass flow forming are increased by 20.41% and 12.58%, respectively.

The variation of the strength of spun tube is corresponding to the decrease of grain size, which has a good agreement with Hall-Petch relationship. In addition, the higher σ_s in RD is resulted from the texture formation. For the peak strength, however, its values in RD are smaller than those in CD. And the strain corresponding to the peak strength in RD is close to each other, while the strain in CD is increased with the thickness reduction. The reason is related to the grain morphology of α grains. After flow forming, the elongated grains are prone to be instable when the grains undergo the compression deformation along RD again. Therefore, when the strain reaches a certain value, approximately 0.35, in this study, the elongated grains are instable and the fracture in the compression samples happens. Since the UFGs microstructures are beneficial for strengthening the samples without any detrimental effect on ductility [29], the peak strength and strain corresponding to the peak strength in CD are increased with the thickness reduction.

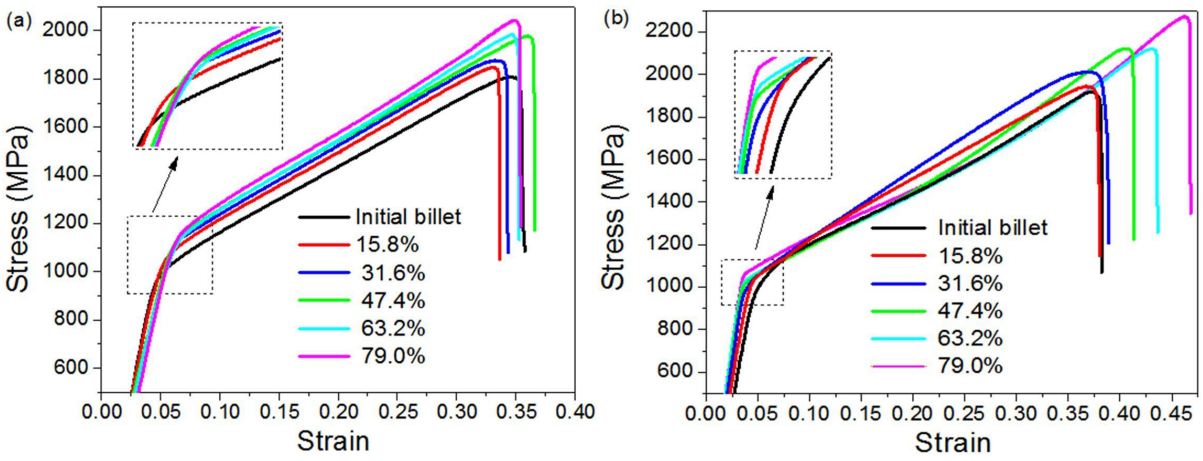

Fig. 11 Variation of the mechanical property of the spun tube in RD (a) and CD (b).

Table 4 Values of σ_s and peak strength in RD and CD.

Thickness reduction ratios	Blank	15.8%	31.6%	47.4%	63.2%	79.0%
σ_s in RD (MPa)	934.58	984.47	1036.98	1057.86	1093.16	1125.3

σ_s in CD (MPa)	939.11	966.32	1007.01	1009.01	1026.91	1057.22
Peak strength in RD (MPa)	1808.41	1846.99	1856.6	1909.41	1895.77	1979.46
Peak strength in CD (MPa)	1833.95	1873.92	1918.7	2010.45	1960.56	2082.09

4. Conclusions

In this study, the microstructure evolution of Ti-6Al-2Zr-1Mo-1V alloy in multi-pass flow forming process is studied and the effect of microstructure evolution on mechanical properties of the spun tube is investigated. The main conclusions are as follows:

(1) Under the influence of the predominant compressive in normal direction (ND) during flow forming process, α grains are flattened in ND and elongated in rolling direction (RD) with the increase of deformation. The kinked grains are occurred in the second and third passes due to the difference in stability of compression in RD between the elongated and equiaxed grains and then gradually disappeared after the fourth pass.

(2) With the increase of deformation, non-standard {0002} basal plane texture is gradually formed with the increase of deformation, which {0002}-poles are titled to circumferential direction (CD) and RD with angles of 20° and 30° and $\{10\bar{1}0\}$-poles are rotated to CD and RD with an angle of 70° and 60°, respectively. The deflection of the non-standard {0002} basal plane is resulted from the significant shear deformation in CD and RD in flow forming process.

(3) After five-pass flow forming, the average size of α grains can be refined to approximately 2μm while the original grain size is 3.75μm. There are two mechanisms for grain refinement, viz., continuous dynamic recrystallization (CDRX)

and deformation-induced intense and localized shearing (DILS). Grains refined by DILS have the different orientation form the non-standard {0002} texture, which can promote the further deformation. For the primary α grains, grain subdivision is mainly achieved by CDRX under small deformation and by DILS under the larger deformation. While both mechanisms have significant effects on the grain refinement of secondary α grains during the whole process.

(4) Compared with the yield strength ($\sigma_{s)}$ of initial billet, the average values of σ_s in RD and CD after five-pass flow forming are improved by 20.41% and 12.58% due to the grain refinement. The peak strength and strain corresponding to the peak strength in CD are increased with the thickness reduction. The values of the peak strength in RD are smaller than those in CD since the elongated grains are prone to be instable when the grains undergo the compression deformation along RD again.

In addition, the understanding of microstructure evolution in multi-pass flow forming process provide a technical guidance for better tailoring of the quality and property of the spun tube and thus it is of importance in design of flow forming process and control and tailoring of the desirable properties of the deformed products.

Acknowledgements

The authors would like to acknowledge the financial support from the National Science Fund for Distinguished Young Scholars of China (No. 51625505), Key Program Project of the Joint Fund of Astronomy and National Natural Science Foundation of China (No. U1537203), and the Research Fund of the State Key Laboratory of Solidification Processing (No. 97-QZ-2014 and 90-QP-2013).

References

[1] D. He, J.C. Zhu, Z.H. Lai, Y. Liu, X.W. Yang, An experimental study of deformation mechanism and microstructure evolution during hot deformation of Ti-6Al-2Zr-1Mo-1V alloy, Mater. Des. 46 (2013) 38-48.

[2] C. Leyens, M. Peters, Titanium and Titanium Alloy, Wiley-VCH, Weinheim, 2003.

[3] M.J. Donachie, Titanium- A Technical Guide, second ed.,ASME International, Metals Park, OH, 1988.

[4] C.C Wong, T. A Dean, J Lin, A review of spinning, shear forming and flow forming processes, Int. J. Mach. Tool Manu. 43 (2003) 1419-1435.

[5] O. Music, J.M. Allwood, K. Kawai, A review of the mechanics of metal spinning, J. Mater. Process. Technol. 210 (2010) 3-23.

[6] Q.X. Xia, G.F. Xiao, H. Long, X.Q. Cheng, X.F. Sheng, A review of process advancement of novel metal spinning, Int. J. Mach. Tool Manu. 85 (2014) 100-121.

[7] I. Weiss, S.L. Semiatin, Thermomechanical processing of alpha titanium alloys-an overview, Mater. Sci. Eng. A 263 (1999) 243-256.

[8] I. Weiss, E.H. Froes, D. Eylon, G.E. Welsch, Modification of alpha morphology in Ti-6AI-4V by thermomechanical processing, Metall. Mater. Trans. A (1985) 1935-1947.

[9] S.L. Semiatin, V. Seetharaman, I. Weiss, The Thermomechanical processing of alpha/beta titanium alloys, JOM 49 (1997) 33-39.

[10] P.F. Gao, H. Yang, X.G. Fan, S.L. Yan, Microstructural features of TA15 titanium alloy under different temperature routes in isothermal local loading forming, Mater. Sci. Eng. A 540 (2012) 245-252.

[11] T. Seshacharyulu, S.C. Medeiros, W.G. Frazier, Y.V.R.K. Prasad, Microstructural mechanisms during hot working of commercial grade Ti-6Al-4V with lamellar starting structure, Mater. Sci. Eng. A 325 (2002) 112-125.

[12] T. Seshacharyulu, S.C. Medeiros, J.T. Morgan, J.C. Malas, W.G. Frazier, Y.V.R.K. Prasad, Hot deformation mechanisms in ELI grade Ti-6A1-4V, Scripta Mater. 41 (1999) 283-288.

[13] T. Seshacharyulu, S.C. Medeiros, J.T. Morgan, J.C. Malas, W.G. Frazier, Y.V.R.K. Prasad, Hot deformation and microstructural damage mechanisms in extra-low interstitial (ELI) grade Ti-6Al-4V, Mater. Sci. Eng. A 279 (2000) 289-299.

[14] M. Zhan, Q.L. Wang, D. Han, H. Yang, Geometric precision and microstructure evolution of TA15 alloy by hot shear spinning, Trans. Nonferrous Met. Soc. China 23 (2013) 1617-1627.

[15] D.B. Shan, G.P. Yang, W.C. Xu, Deformation history and the resultant microstructure and texture in backward tube spinning of Ti-6Al-2Zr-1Mo-1V, J. Mater. Process. Technol. 209 (2009) 5713-5719.

[16] Y Chen, W.C. Xu, D.B. Shan, B. Guo, Microstructure evolution of TA15 titanium alloy during hot power spinning, Trans. Nonferrous Met. Soc. China 21 (2011) 323-327.

[17] W.C. Xu, C. Wen, D.B. Shan, Z.L. Wang, G.P. Yang, Y. Lu, Effect of spinning deformation on microstructure evolution and mechanical property of TA15 titanium alloy, Trans. Nonferrous Met. Soc. China 17 (2007) 1205-1211.

[18] S. Roy, S. Suwas, The influence of temperature and strain rate on the deformation response and microstructural evolution during hot compression of α titanium alloy

Ti-6Al-4V-0.1B, J. Alloys Comp. 548 (2013), 110-125.

[19] S. Zaefferer, A study of active deformation systems in titanium alloys: dependence on alloy composition and correlation with deformation texture, Mater. Sci. Eng. A 344 (2003) 20-30.

[20] E. Tenckhoff, Verformungsmechanismen, Textur und Anisotropie in Zirkonium und Zircaloy, Materialkundlich-Technische Reihe 5, Gebr. Borntrager, Berlin, 1980.

[21] F. Bridier, P. Villechaise, J. Mendez, Analysis of the different slip systems activated by tension in a α/β titanium alloy in relation with local crystallographic orientation, Acta Mater. 53 (2005) 555-567.

[22] J.C. Williams, R.G. Baggerly, N.E. Paton, Deformation behavior of HCP Ti-Al alloy single crystals, Metall. Mater. Trans. A 33 (2002) 837-850.

[23] J. Guo, M. Zhan, H. Yang, Analysis of shearing deformation in rolling-spinning forming of Ti-6Al-2Zr-1Mo-1V tubes, MATEC Web of Conferences, Glasgow, 21 (2015).

[24] Q.X Xia, G.F Xiao, H. Long, X. Cheng, B.J. Yang, A study of manufacturing tubes with nano/ultrafine grain structure by stagger spinning, Mater. Des. 59 (2014) 516-523.

[25] M. Zhan, X.X. Wang, H. Long, Mechanism of grain refinement of aluminium alloy in shear spinning under different deviation ratios, Mater. Des. 108 (2016) 207-216.

[26] F.J Humphreys, M. Hatherly, Recrystallization and Related Annealing Phenomena, second ed., Oxford: Elsevier, 2004.

[27] T. Saka, A. Belyakov, R. Kaibyshev, H. Miura, J.J. Jonas, Dynamic and post-dynamic recrystallization under hot, cold and severe plastic deformation conditions, Prog. Mater. Sci. 60 (2014) 130-207.

[28] S. Mironov, M. Murzinova, S. Zherebtsov, G.A. Salishchev, S.L. Semiatin, Microstructure evolution during warm working of Ti-6Al-4V with a colony-a microstructure, Acta Mater. 57 (2009) 2470-2481.

[29] S. Zherebtsov, M. Murzinova, G. Salishchev, S.L. Semiatin, Spheroidization of the lamellar microstructure in Ti-6Al-4V alloy during warm deformation and annealing, Acta Mater. 59 (2011) 4138-4150.

[30] S.L. Semiatin, T.R. Bieler, The effect of alpha platelet thickness on plastic flow during hot working of Ti-6Al-4V with a transformed microstructure, Acta Mater. 49 (2001) 3565-3573.

[31] S. Zherebtsov, E. Kudryavtsev, S. Kostjuchenko, S. Malysheva, G. Salishchev, Strength and ductility-related properties of ultrafine grained two-phase titanium alloy produced by warm multiaxial forging, Mater. Sci. Eng. A 536 (2012) 190-196.